

Association of Respiratory Functional Indices and Smoking with Pleural Movement and Mean Lung Density Assessed Using Four-Dimensional Dynamic-Ventilation Computed Tomography in Smokers and Patients with COPD

Ryo Uemura¹, Yukihiro Nagatani¹, Masayuki Hashimoto^{2,3}, Yasuhiko Oshio³, Akinaga Sonoda¹, Hideji Otani¹, Jun Hanaoka³, Yoshiyuki Watanabe¹

¹Department of Radiology, Shiga University of Medical Science, Otsu, Shiga, Japan; ²Department of Thoracic Surgery, Kyoto Medical Center, Kyoto, Kyoto, Japan; ³Division of General Thoracic Surgery, Department of Surgery, Shiga University of Medical Science, Otsu, Shiga, Japan

Correspondence: Ryo Uemura; Yukihiro Nagatani, Department of Radiology, Shiga University of Medical Science, Seta-tsukinowa-cho, Otsu, Shiga, Japan, 520-2192, Tel/Fax +81-77-548-2536, Email uemurar@belle.shiga-med.ac.jp; yatsushi@belle.shiga-med.ac.jp

Purpose: To correlate the ratio of the non-dependent to dependent aspects of the maximal pleural movement vector (MPMV_{ND/D}) and gravity-oriented collapse ratio (GCR_{ND/D}), and the mean lung field density (MLD) obtained using four-dimensional (4D) dynamic-ventilation computed tomography (DVCT) with airflow limitation parameters and the Brinkman index.

Materials and Methods: Forty-seven patients, including 22 patients with COPD, 13 non-COPD smokers, and 12 non-smokers, with no/slight pleural adhesion confirmed using a thoracoscope, underwent 4D-DVCT with 16 cm coverage. Coordinates for the lung field center, as well as ventral and dorsal pleural points, set on the central trans-axial levels in the median and para-median sagittal planes at end-inspiration, were automatically measured (13–17 frame images, 0.35 seconds/frame). MPMV_{ND/D} and GCR_{ND/D} were calculated based on MPMV and GCR values for all the included points and the lung field center. MLD was automatically measured in each of the time frames, and the maximal change ratio of MLD (MLD_{CR}) was calculated. These measured values were compared among COPD patients, non-COPD smokers, and non-smokers, and were correlated with the Brinkman index, FEV₁/FVC, FEV₁ predicted, RV/TLC, and FEF_{25–75%} using Spearman's rank coefficients.

Results: MPMV_{ND/D} was highest in non-smokers (0.819±0.464), followed by non-COPD smokers (0.405±0.131) and patients with COPD (−0.219±0.900). GCR_{ND/D} in non-smokers (1.003±1.384) was higher than that in patients with COPD (−0.164±1.199). MLD_{CR} in non-COPD smokers (0.105±0.028) was higher than that in patients with COPD (0.078±0.027). MPMV_{ND/D} showed positive correlations with FEV₁ predicted ($r=0.397$, $p=0.006$), FEV₁/FVC ($r=0.501$, $p<0.001$), and FEF_{25–75%} ($r=0.368$, $p=0.012$). GCR_{ND/D} also demonstrated positive correlations with FEV₁ ($r=0.397$, $p=0.006$), FEV₁/FVC ($r=0.445$, $p=0.002$), and FEF_{25–75%} ($r=0.371$, $p=0.011$). MPMV_{ND/D} showed a negative correlation with the Brinkman index ($r=-0.398$, $p=0.006$).

Conclusion: We demonstrated that reduced MPMV_{ND/D} and GCR_{ND/D} were associated with respiratory functional indices, in addition to a negative association of MPMV_{ND/D} with the Brinkman index, which should be recognized when assessing local pleural adhesion on DVCT, especially for ventral pleural aspects.

Keywords: chronic obstructive pulmonary disease, smoking burden, four-dimensional dynamic-ventilation computed tomography, pleural movement, mean lung density, gravity-oriented distance

Introduction

In chronic obstructive pulmonary disease (COPD), a flattened diaphragm is associated with lung hyperinflation, which can lead to asynchronous movement of the chest wall with negative impacts on ventilatory mechanics.¹ Following

perceptives of movement impairment in the diaphragm or lung parenchyma have been obtained using dynamic imaging modalities. Paradoxical diaphragmatic motion that the diaphragm moves downward as the lung volume decreases was reported to be observed in patients with COPD based on the visual assessment of dynamic magnetic resonance imaging (MRI) images. The measurement of paradoxical diaphragmatic motion was correlated with forced expiratory volume in 1 second (FEV₁), FEV₁/forced vital capacity (FVC), and emphysema of the lower lung zone.² Moreover, in paired computed tomography (CT) series in the deep-inspiratory and deep-expiratory states, mean lung parenchymal movement vectors in the ventrodorsal and craniocaudal directions correlated well with respiratory functional indices.³ Heterogeneity in airflow obstruction distribution and lung parenchymal motion in smokers with/without COPD can be reflected in these results. It is unclear how these abnormal movements of the diaphragm and lung parenchyma, or localized collapse of the lung field due to a decrease in surfactant associated with smoking, affect the subpleural lung field and pleural movements.

The use of video-assisted thoracoscopic surgery (VATS) for the resection of thoracic malignant tumors has increased,^{4,5} mainly because of its better outcomes compared to thoracotomy.^{6–8} However, in some cases, unexpected conversions from VATS to thoracotomy are required owing to some surgical conditions, including severe localized pleural adhesion (LPA).⁹ Therefore, the preoperative recognition of LPA is desirable. Invasion of lung cancer to the chest wall has been feasibly visualized on four-dimensional (4D) dynamic-ventilation computed tomography (DVCT) with standard dose settings.¹⁰ There remain concerns over daily clinical examination for the detection of LPA owing to the relatively high radiation exposure of DVCT. Ultra-low-dose CT has demonstrated comparable image quality, such as lung nodule detection performance, to low-dose CT in combination with an iterative reconstruction algorithm,^{11–15} with sufficient visibility of peripheral lung vessels. Thus, even DVCT at an ultra-low-dose setting can increase the detection sensitivity with suppress false-negative cases as far as possible in terms of the detection of LPA, compared with conventional static images.¹⁶ LPA was demonstrated to be detected more often by referring to a three-dimensional color map generated using software-assisted analysis, which predicted the amount of sliding pleura against the chest wall.¹⁷ However, LPA detectability has not yet been improved enough to reach a satisfactory level.

Therefore, if we demonstrate associations between pleural movement and smoking or respiratory functional indices in cases without adhesion, it will provide a considerable advance in the establishment of an automatic detection algorithm for LPA.

Thus, the purpose of this study was to quantify pleural movement and changes in both mean lung field density (MLD) and distance in the gravitational direction during respiration on DVCT, and to assess their correlations with respiratory functional indices and smoking.

Materials and Methods

The institutional review board of our institution approved this study. In this study, written informed consent from all included patients was obtained, in accordance with the ethical standards laid down in the Declaration of Helsinki. This research was retrospectively performed as an additional evaluation after our previous research, which focused on assessing the ability of DVCT to detect LPA by measuring respiratory change in the distance between the pleura and chest wall.¹⁶ This research was also arranged as part of the Area-detector Computed Tomography for the Investigation of Thoracic Diseases (ACTive) study, a Japanese multicenter research project in progress for 10 years or more, on the basis of its research committee.

Selection Process of Study Population

We retrospectively analyzed 22 patients with COPD, 13 non-COPD smokers (NCS), and 12 non-smokers (NS) extracted from 69 consecutive patients who underwent DVCT within a week prior to lung surgery from November 2015 to November 2016 and had no or minor pleural adhesions confirmed at surgery. Patients with some history of smoking exposure were defined as smokers, regardless of smoking cessation. In the NCS group, 38% of patients were current smokers, whereas 23% of patients were current smokers in the COPD group. The continuing and cessation durations of smoking exposure for COPD were similar to those of NCS, as the continuing period of smokers and smoking cessation duration of ex-smokers were 38.3±13.3 years and 16.4±10.8 years for COPD, and 38.8±12.8 years and 15.6±13.1 years

for NCS, respectively. The cases of two COPD patients and one NCS patient were complicated by smoking-related interstitial lung disease. Table 1 summarizes the patient characteristics. Four patients in the COPD group underwent thoracotomy, due to tracheoplasty being required as a result of the tumor location involving the central airways (n=1) and preoperative estimation of pleural adhesion by larger subpleural lung tumors, to some extent (n=3). The remaining 43 patients underwent VATS. The types of surgery are summarized in Table 2.

Table 1 Patients' Characteristics

	Total Population	COPD	Non-COPD Smoker	Non-Smoker
Age (years)	70.6±9.3	74.1±6.1 ^a	68.2±4.9	66.9±14.8
Gender (F/M)	21/26	8/14	2/11	11/1 ^b
Height (cm)	160.2±8.1	160.0±8.1	165.1±5.2 ^c	155.2±7.9
Body weight (kg)	58.4±12.2	57.4±11.0	68.1±10.6 ^d	49.9±8.9
FEV ₁ /FVC (%)	70.3±10.8	61.6±7.5 ^e	76.9±5.6	79.1±7.6
FEV ₁ predicted (%)	92.5±15.2	84.5±14.8 ^e	96.9±12.2	102.3±11.3
RV (L)	2.0±0.5	2.1±0.4	2.3±0.5	1.7±0.3 ^f
TLC (L)	5.1±1.1	5.3±1.0	5.8±1.0	4.2±0.6 ^f
RV/TLC (%)	40.1±5.4	40.2±5.6	39.8±4.1	40.1±6.1
FEF _{25-75%}	1.5±0.8	0.9±0.4 ^e	2.2±0.9	1.8±0.6
Smoking exposure				
Current smoker	10	5	5	0
Ex-smoker	23	15	8	0
Brinkman index	605.9±600.4	759.9±604.2	904.6±485.5	0.0±0.0 ^f
Maximal MLD	-750.6±43.7	-760.5±31.8	-736.7±59.1	-747.4±42.7
Minimal MLD	-825.2±35.8	-825.5±30.3	-816.4±49.8	-834.2±26.6

Notes: ^aHigher than non-COPD smoker; ^bMore women were included; ^cHigher than non-smoker; ^dLarger than both COPD and non-smoker; ^eLower than both non-COPD smoker and non-smoker; ^fLower than both COPD and non-COPD smoker.
Abbreviations: COPD, chronic obstructive pulmonary disease; FEV₁, forced expiratory volume in 1 second; FVC, forced vital capacity; RV, residual volume; TLC, total lung capacity; FEF_{25-75%}, forced mid-expiratory flow; MLD, mean lung density.

Table 2 Operative Procedure

	Total Population	COPD	Non-COPD Smoker	Non-Smoker
Type of surgery				
Thoracotomy	4	4	0	0
VATS	43	18	13	12
Lobectomy	26	16	7	3
Segmentectomy	6	1	1	4
Partial resection	15	5	5	5

Abbreviations: VATS, video-assisted thoracoscopic surgery; COPD, chronic obstructive pulmonary disease.

Dynamic-Ventilation Computed Tomography

The included patients underwent DVCT sequentially after our preoperative routine chest CT series, as follows. Initially, a scanning area with Z-axis coverage of 16 cm was set to include entire pulmonary target lesions. Second, the patients were asked to breathe in accordance with a predefined constant respiratory cycle. Third, the patient's breathing was confirmed to be synchronous with the respiratory cycle. Finally, dynamic image data were obtained for 5.29 ± 0.31 seconds during at least a single respiration in a wide volume scanning mode with a 320-row CT scanner (Aquilion ONE; Canon Medical Systems, Otawara, Tochigi, Japan).

In this study, dynamic imaging data were obtained at a tube current of 20 mA, tube voltage of 120 kVp, rotation time of 0.35 seconds, field of view (FOV) of 320 mm, and collimation and slice thickness of 0.5 mm. Several reconstruction parameters were adopted as follows: collimation and slice thickness of 0.5 mm, standard kernel (FC13), interval of 0.35 second per frame, and full reconstruction method. Calculation of the effective dose was based on the multiplication of the dose-length product values, based on the CT dose index volume, by a factor of 0.014.¹⁸

Image Analysis: Mean Lung Field Density Measurement on Dynamic-Ventilation Computed Tomography

A previous study showed an excellent correlation in the change in mean lung density (MLD) with that in total lung volume (TLV) between inspiratory and expiratory CT.¹⁹ Moreover, a systematic review and meta-analysis confirmed that MLD was related to airflow obstruction assessed using FEV_1 %predicted and FEV_1/FVC , in patients with COPD.²⁰ Therefore, in cases where only part of the TLV is available for dynamic imaging data, as in this study, MLD can be utilized as an alternative parameter instead of TLV, in an attempt to assess the correlation between the movement of a structure of interest and TLV change.

Using commercially available software (Lung Volume Measurement; Canon Medical Systems), MLD was automatically measured in each time frame, and the time curve of MLD on DVCT images was created. On the time curve, the peak expiratory (maximum) MLD (MLD_{max}), peak inspiratory (minimum) MLD (MLD_{min}), and change ratio of MLD (MLD_{CR} ; defined as the subtracted value of MLD at peak expiration from MLD at peak inspiration divided by MLD at peak inspiration) were obtained.

Image Analysis: Quantitative Assessment of the Movement of Pleura and the Center of the Lung Field during a Single Expiration

At end-inspiration, measurement points were placed at central trans-axial levels across the posterior costal bones on both the dependent pleural aspect (DPA) and non-dependent pleural aspect (NDPA) in the median and para-median sagittal planes (15 mm lateral from the median), except for the pulmonary apical and subphrenic area (Figure 1). The lung field center (LFC) was placed at a central trans-axial level across the median posterior costal bone in the median sagittal plane (Figure 1). These coordinates in the other respiratory phases were determined by automatic tracking functions with minimal manual intervention.

For two measurement points on both the DPA and NDPA at each of the central trans-axial levels, the maximal movement vectors during expiration were measured based on changes in coordinates. The maximal movement vectors in the caudocranial and craniocaudal directions were defined as positive and negative values, respectively. The mean value of the relative proportion of NDPA to DPA in the maximal movement vector among all of the measurement points was calculated and defined as the non-dependent to dependent ratio in the maximal pleural movement vector ($MPMV_{ND/D}$).

For each of the measurement points in the median sagittal plane on either the DPA or NDPA, the maximal decrease ratio during expiration in the gravity-oriented distance to the LFC (defined as the maximal decrease distance divided by the distance at peak inspiration) was measured. The mean value of the relative proportion of NDPA to DPA in the maximal decrease ratio among all of the measurement points was calculated and defined as the non-dependent to dependent ratio in the gravity-oriented collapse ratio ($GCR_{ND/D}$).

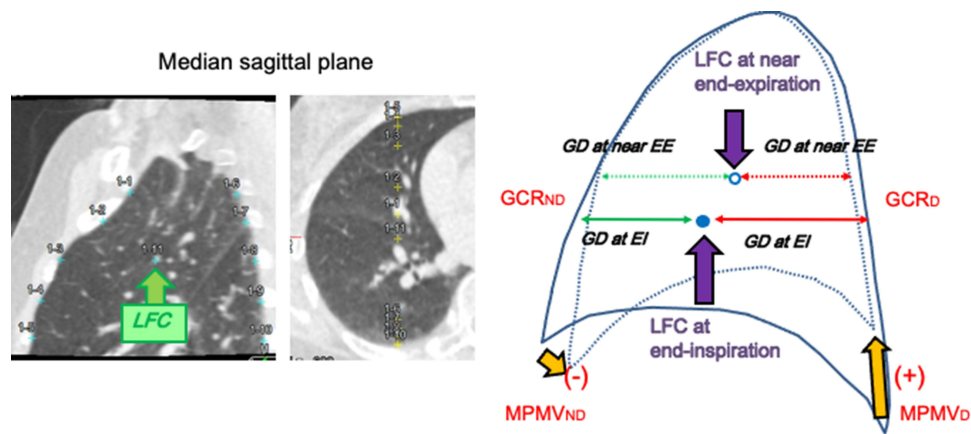


Figure 1 Example images of point placement at end-inspiration for quantitative measurement of the movement of pleura and lung field center during a single respiration, and a scheme for measured values for pleural movement and gravity-oriented distance. Example images for measurement point replacements at end-inspiration in both non-dependent and dependent pleural aspects at the costal central levels in the dependent pleural aspect and for the lung field center in the median planes, except for pulmonary apical regions, are shown on the left. Their coordinates in the remaining respiratory phases were determined by automatic tracking functions with minimal manual intervention. As shown in the scheme on the right, MPMVs in the cranial direction were defined as positive. In addition, GCR was defined as the subtracted value of the GD at peak expiration from the GD at peak inspiration divided by the GD at peak inspiration. MPMV and GCR were measured in the non-dependent and dependent pleural aspects, respectively.

Abbreviations: LFC, lung field center; GD, gravity-oriented distance; EE, end-expiration; EI, end-inspiration; GCR_{ND}, gravity-oriented collapse ratio in the non-dependent aspect; GCR_D, gravity-oriented collapse ratio in the dependent aspect; MPMV_{ND}, mean value of the ratio of the maximal pleural movement vectors in the non-dependent aspect; MPMV_D, mean value of the ratio of the maximal pleural movement vectors in the dependent aspect.

Pulmonary Function Evaluation

Within a month of the DVCT examination, all of the included patients underwent spirometry, including FEV₁, FVC, residual volume (RV), total lung capacity (TLC), and forced mid-expiratory flow (FEF_{25–75%}), in accordance with the American Thoracic Society standards.

Statistical Analysis

The mean values of MPMV_{ND/D}, GCR_{ND/D}, and MLD parameters (MLD_{max}, MLD_{min}, and MLD_{CR}) were positive. MPMV_{ND/D}, GCR, and MLD parameters were compared among the three groups (patients with COPD, NCS, and NS) using the Kruskal-Wallis and Mann-Whitney Utests. Spearman rank correlation analysis was used to estimate the relationships among these measured values obtained using DVCT and quantitative parameters relevant to smoking and airflow limitation.

Results

Comparison of MPMV_{ND/D} and GCR_{ND/D} Among Patients with COPD, Non-COPD Smokers, and Non-Smokers

MPMV_{ND/D} was highest in the NS group (0.819±0.464), followed by the NCS group (0.405±0.131) and patients with COPD (−0.219±0.900). GCR_{ND/D} in the NS group (1.003±1.384) was higher than that in patients with COPD (−0.164±1.199) (Figure 2).

Comparison of MLD Parameters Among Patients with COPD, Non-COPD Smokers, and Non-Smokers

MLD_{CR} in the NCS group (0.105±0.028) was higher than that in patients with COPD (0.078±0.027). No significant difference was found in MLD_{max} and MLD_{min} among the three groups (Figure 2).

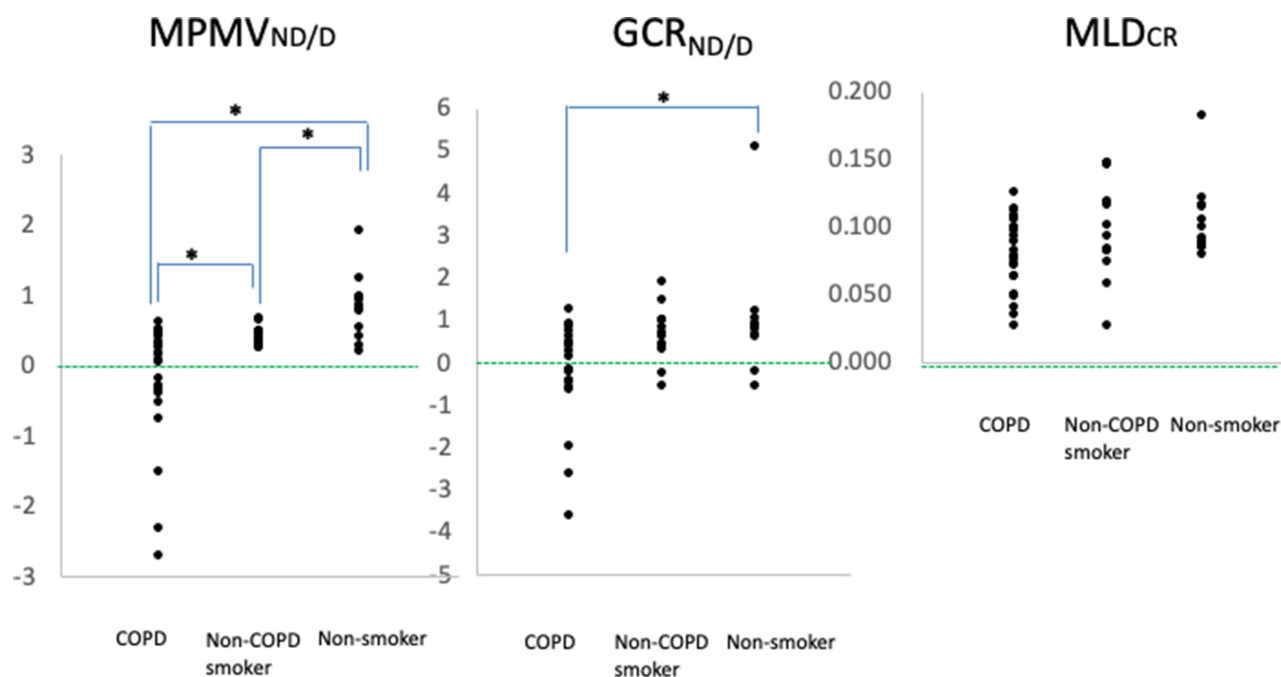


Figure 2 Comparison of $MPMV_{ND/D}$, $GCR_{ND/D}$, and MLD_{CR} among COPD patients, non-COPD smokers, and non-smokers. Dot-plot graphs show differences in the distribution for $MPMV_{ND/D}$, $GCR_{ND/D}$, and MLD_{CR} among patients with COPD and the non-COPD smoker and non-smoker groups. $MPMV_{ND/D}$ was highest in the non-smoker group (0.819 ± 0.464), followed by the non-COPD smoker group (0.405 ± 0.131) and patients with COPD (-0.219 ± 0.900). $GCR_{ND/D}$ in the non-smoker group (1.003 ± 1.384) was higher than that in patients with COPD (-0.164 ± 1.199). MLD_{CR} in the non-COPD smoker group (0.105 ± 0.028) tended to be higher than in patients with COPD (0.078 ± 0.027).

Abbreviations: $MPMV_{ND/D}$, ratio of the non-dependent to dependent pleural aspects in the maximal pleural movement vector; $GCR_{ND/D}$, ratio of the non-dependent to dependent lung field in the gravity-oriented collapse ratio; MLD_{CR} , change ratio of mean lung density.

Correlation of $MPMV_{ND/D}$ and $GCR_{ND/D}$ with Respiratory Functional Indices and the Brinkman Index

In the total study population, $MPMV_{ND/D}$ showed positive correlation coefficients with FEV_1 predicted ($r=0.397$, $p=0.006$), FEV_1/FVC ($r=0.501$, $p<0.001$), and $FEF_{25-75\%}$ ($r=0.368$, $p=0.012$). $MPMV_{ND/D}$ showed a negative correlation coefficient with the Brinkman index ($r=-0.398$, $p=0.006$), but $GCR_{ND/D}$ did not. $GCR_{ND/D}$ also demonstrated positive correlation coefficients with FEV_1 predicted ($r=0.397$, $p=0.006$), FEV_1/FVC ($r=0.445$, $p=0.002$), and $FEF_{25-75\%}$ ($r=0.371$, $p=0.011$) (Figure 3) (Table 3).

Correlation of MLD Parameters with Respiratory Functional Indices

In the total study population, MLD_{CR} tended to have a positive correlation coefficient with FEV_1/FVC ($r=0.285$, $p=0.052$). Neither RV/TLC nor $FEF_{25-75\%}$ was demonstrated to have an association with MLD_{CR} . No significant correlation was found between either MLD_{max} or MLD_{min} and respiratory functional indices. In addition, there was no significant correlation between MLD parameters and the Brinkman index. Only for the NCS group, MLD_{min} correlated negatively with FEV_1/FVC ($r=-0.560$, $p=0.046$) (Table 4).

Correlation of $MPMV_{ND/D}$ and $GCR_{ND/D}$ with MLD Parameters

A positive correlation coefficient was found between $MPMV_{ND/D}$ and MLD_{CR} ($r=0.327$, $p=0.025$). In addition, $MPMV_{ND/D}$ correlated negatively with MLD min for NCS group ($r = -0.566$, $p= 0.044$).

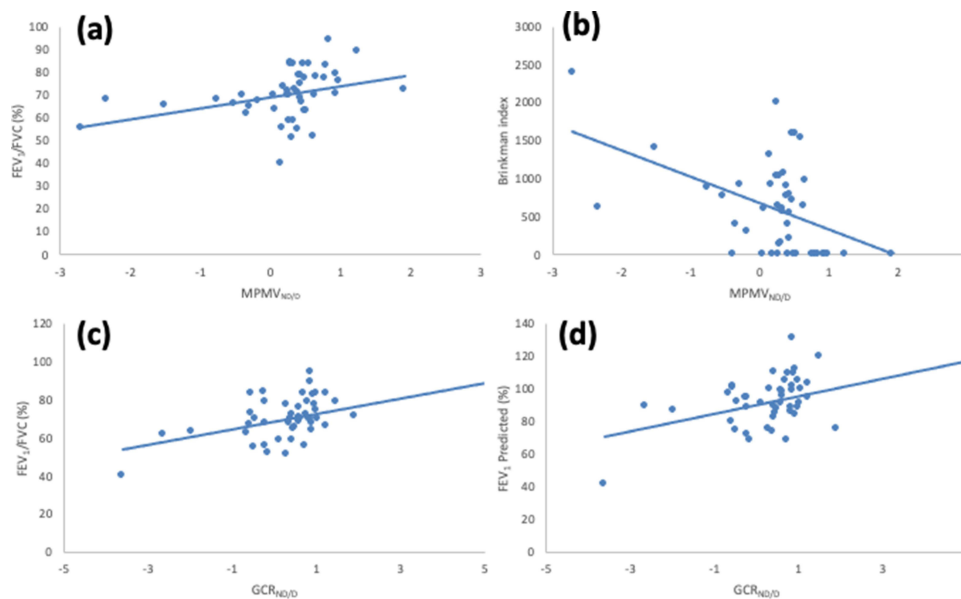


Figure 3 Correlation of $MPMV_{ND/D}$ and $GCR_{ND/D}$ with respiratory functional indices and Brinkman index. Scatterplot graphs for the total study population show the positive association between $MPMV_{ND/D}$ and FEV_1/FVC , with $r=0.501$, $p<0.001$ (a), the negative association between $MPMV_{ND/D}$ and Brinkman index, with $r=-0.398$, $p=0.006$ (b), the positive association between $GCR_{ND/D}$ and FEV_1/FVC , with $r=0.445$, $p=0.002$ (c), and the positive association between $GCR_{ND/D}$ and FEV_1 predicted, with $r=0.397$, $p=0.006$ (d). The mean values were distributed around straight lines in each graph, given by $y=4.85x+69.2$, $y=-347x+682$, $y=4.03x+68.8$, and $y=5.34x+90.5$, respectively.

Abbreviations: FEV_1 , forced expiratory volume in 1 second; FVC, forced vital capacity; $MPMV_{ND/D}$, ratio of the non-dependent to dependent pleural aspects in the maximal pleural movement vector; $GCR_{ND/D}$, ratio of the non-dependent to dependent lung field in the gravity-oriented collapse ratio.

Estimated Radiation Dose

For a single gantry rotation of 160 mm during 0.35 seconds, the volume computed tomography dose index ($CTDI_{vol}$) was 0.504 mGy. The dose length product (DLP) value for a single rotation was 8.06 mGy cm. The total estimated radiation exposure for DVCT for 4.2–6.0 seconds was 1.64–2.32 mSv (2.07 ± 0.12 mSv).

Discussion

In this study, we compared quantitative measured values of pleural movements, collapse of lung fields in the gravitational direction, and MLD changes on DVCT images among three groups classified according to the presence of airflow limitation and smoking habits, comprising 22 patients with COPD, 13 in the NCS group, and 12 in the NS group, and correlated these measured values with airflow limitation parameters assessed using pulmonary function tests and the Brinkman smoking index. We found that: 1) $MPMV_{ND/D}$ was different among the three groups, and correlated positively with FEV_1 predicted, FEV_1/FVC , and $FEF_{25-75\%}$, as well as MLD_{CR} , and negatively with the Brinkman index; and 2) $GCR_{ND/D}$ in patients with COPD was lower than that in the NS group, and correlated positively with FEV_1 predicted, FEV_1/FVC , and $FEF_{25-75\%}$ (Figure 4).

$MPMV_{ND/D}$ was largest in the NS group, followed by the NCS group and patients with COPD. Smaller $MPMV_{ND/D}$ values indicate that pleural movement in the non-dependent aspect becomes smaller or moves in opposite direction compared with the dependent aspect (Figure 4). $MPMV_{ND/D}$ correlated positively with airflow limitation parameters in pulmonary function tests and negatively with the smoking index, which suggested that cumulative smoking burden, as well as airflow limitation, correlated with a relative decrease in pleural movement in the non-dependent aspect or a relative increase in pleural movement in the dependent aspect during breathing. Based on data analysis of DVCT, a previous study reported reduced movement in the peripheral parenchyma of the lung field adjacent to the non-dependent aspect at the level of the diaphragm in patients with COPD compared with those with asthma.²¹

Another previous study demonstrated that airflow limitation causes heterogeneous interlobar respiratory changes in MLD that reflect lung volume.²² These results can reflect regional discordance in respiratory movements in COPD. Also in this study, $GCR_{ND/D}$, as well as $MPMV_{ND/D}$, correlated positively with FEV_1 predicted, FEV_1/FVC , and $FEF_{25-75\%}$.

Table 3 Correlation of Measured Values with Respiratory Functional Indices and Brinkman Index

	FEV ₁ /FVC		FEV ₁ Predicted		Brinkman Index		RV/TLC		FEF _{25-75%}	
	r-value	p-value	r-value	p-value	r-value	p-value	r-value	p-value	r-value	p-value
Total study population										
MPMV _{ND/D}	0.501	<0.001	0.397	0.006	-0.398	0.006	-0.123	0.445	0.368	0.012
GCR _{ND/D}	0.445	0.002	0.397	0.006	-0.202	0.172	0.179	0.264	0.371	0.011
COPD										
MPMV _{ND/D}	-0.351	0.109	-0.079	0.726	-0.109	0.629	-0.275	0.240	-0.241	0.281
GCR _{ND/D}	-0.034	0.879	-0.178	0.427	-0.012	0.956	0.215	0.363	0.305	0.167
Non-COPD smoker										
MPMV _{ND/D}	0.060	0.845	0.399	0.177	-0.225	0.459	-0.418	0.229	0.273	0.391
GCR _{ND/D}	0.286	0.344	-0.066	0.830	0.363	0.223	0.442	0.200	-0.231	0.471
Non-smoker										
MPMV _{ND/D}	0.161	0.618	0.228	0.477	N/A	N/A	0.191	0.574	-0.007	0.983
GCR _{ND/D}	-0.014	0.966	-0.501	0.097	N/A	N/A	-0.182	0.593	0.161	0.618

Note: Significant values are shown in bold.

Abbreviations: FEV₁, forced expiratory volume in 1 second; FVC, forced vital capacity; MPMV_{ND/D}, ratio of the non-dependent to dependent aspects in the maximal pleural movement vector; GCR_{ND/D}, ratio of the non-dependent to dependent pleural aspects in the gravity-oriented collapse ratio; COPD, chronic obstructive pulmonary disease; RV, residual volume; TLC, total lung capacity; FEF_{25-75%}, forced mid-expiratory flow.

Considering that smaller GCR_{ND/D} means impairment of volume reduction during expiration in the gravitational direction, this result suggests that the relative decrease in non-dependent lung field movement associated with airflow limitation correlated with the relative restriction of pleural movement in the non-dependent aspect, and we consider that this is a new perspective obtained from the analysis of DVCT. In this study, some patients with COPD showed paradoxical movement of the non-dependent pleura in the craniocaudal direction during expiration (Figure 5) (Video S1), which is consistent with paradoxical movement of the diaphragm in the non-dependent aspect in patients with COPD, as demonstrated using cine images of MRI.² Data analysis of DVCT with a fixed sized volume of interest demonstrated that MLD increased in the right lower lobe, whereas MLD decreased in the right upper and middle lobes during expiration in some patients with COPD, which may reflect a phenomenon of paradoxical volume increase during expiration because of patent collateral ventilation in the periphery with relatively strong expiratory obstruction of the central airways.²² These findings are consistent with the craniocaudal movement of the pleura in the non-dependent aspect associated with airflow limitation demonstrated in this study. On the other hand, RV/TLC was not shown to be associated with either MPMV_{ND/D} or GCR_{ND/D} in this study, although RV/TLC has been reported to be a reproducible and reliable parameter in the assessment of static lung hyperinflation, which can be a determining factor of exercise tolerance and quality of life, regardless of the difference in measurement tools.²³ The lack of association of MPMV_{ND/D} and GCR_{ND/D} with RV/TLC could be explained by the fact that the first two parameters were obtained during total expiration, which can reflect dynamic and regional lung hyperinflation, where RV and TLC were measured at peak expiration and peak inspiration, respectively, and are representative of static ventilation parameters. In addition, the presence of emphysema and conventional static lung hyperinflation parameters, such as the percentage of low attenuation area less than -950 HU, was also demonstrated to be associated with an increased risk of postoperative respiratory failure in cases with lung cancer.²⁴

This study also demonstrated that pleural movement in the dependent aspect was larger than in the non-dependent aspect, even in smokers without airflow limitation compared with non-smokers (Figures 6 and 7) (Videos S2 and S3). Furthermore, MPMV_{ND/D} decreased as MLD at maximum as inspiration increased; in other words, the extent/degree of lung parenchymal collapse at peak inspiration became larger in smokers, especially for the dependent lung field.

Table 4 Correlation of Mean Lung Density Parameters with Respiratory Functional Indices and Brinkman Index

	FEV ₁ /FVC		FEV ₁ Predicted		Brinkman Index	
	r-value	p-value	r-value	p-value	r-value	p-value
<i>Total study population</i>						
MLD _{max}	0.117	0.435	0.022	0.882	0.117	0.434
MLD _{min}	-0.024	0.875	-0.099	0.507	0.227	0.125
MLD _{CR}	0.285	0.052	0.265	0.072	-0.209	0.158
<i>COPD</i>						
MLD _{max}	0.184	0.414	0.083	0.713	0.014	0.952
MLD _{min}	0.141	0.531	-0.193	0.390	0.133	0.556
MLD _{CR}	0.019	0.934	0.344	0.117	-0.141	0.531
<i>Non-COPD smoker</i>						
MLD _{max}	-0.264	0.384	-0.498	0.083	0.286	0.344
MLD _{min}	-0.560	0.046	-0.413	0.161	0.236	0.437
MLD _{CR}	0.027	0.929	-0.256	0.399	-0.049	0.873
<i>Non-smoker</i>						
MLD _{max}	0.000	1.000	0.553	0.062	N/A	N/A
MLD _{min}	-0.042	0.897	0.518	0.084	N/A	N/A
MLD _{CR}	-0.161	0.618	0.168	0.601	N/A	N/A

Note: Significant values are shown in bold.

Abbreviations: FEV₁, forced expiratory volume in 1 second; FVC, forced vital capacity; COPD, chronic obstructive pulmonary disease; MLD_{CR}, change ratio in mean lung density during expiration.

Considering that smokers without airflow limitation in this study had no apparent emphysematous changes, this result indicated that a relatively large pleural movement in the dependent aspect during expiration, compared with the non-dependent aspect, may be associated with stronger collapse of the dependent lung fields at peak inspiration. Moreover, data analysis of DVCT obtained in the lateral position demonstrated that MLD at peak inspiration in the dependent lung field was higher by 40 HU than in the non-dependent lung field.²⁵ Considering the preserved association between central airway dimension and MLD in the dependent lung field in the NCS group, relatively large pleural movements in the dependent aspect may be a complementary phenomenon to preserve ventilation within the normal range, even in parenchymal regions with collapse, to some extent.

Based on these findings on the reduction in movement in the ventral pleural aspects for the NCS group and patients with COPD, we should pay attention to potential overestimation of the presence of LPA in ventral aspects for smokers with visual evaluation on DVCT. In addition, weighting factors of lung parenchymal movements in the periphery against chest wall movements should be appropriately adjusted in the ventral pleural aspects to enable the improvement of automatic detection algorithms for LPA.

In this study, we used MLD as an alternative parameter instead of TLV because part of the lung field is outside the fixed scanning range with 16 cm coverage in the craniocaudal direction on DVCT. Because a strong positive correlation was reported between MLD and TLV in a previous study,¹⁹ MLD_{CR} is considered to reflect changes in TLV during respiration. Most previous reports demonstrated correlations between expiratory MLD and respiratory functional indices; however, another study demonstrated a correlation between the change ratio of inspiration to expiration in MLD and parameters in

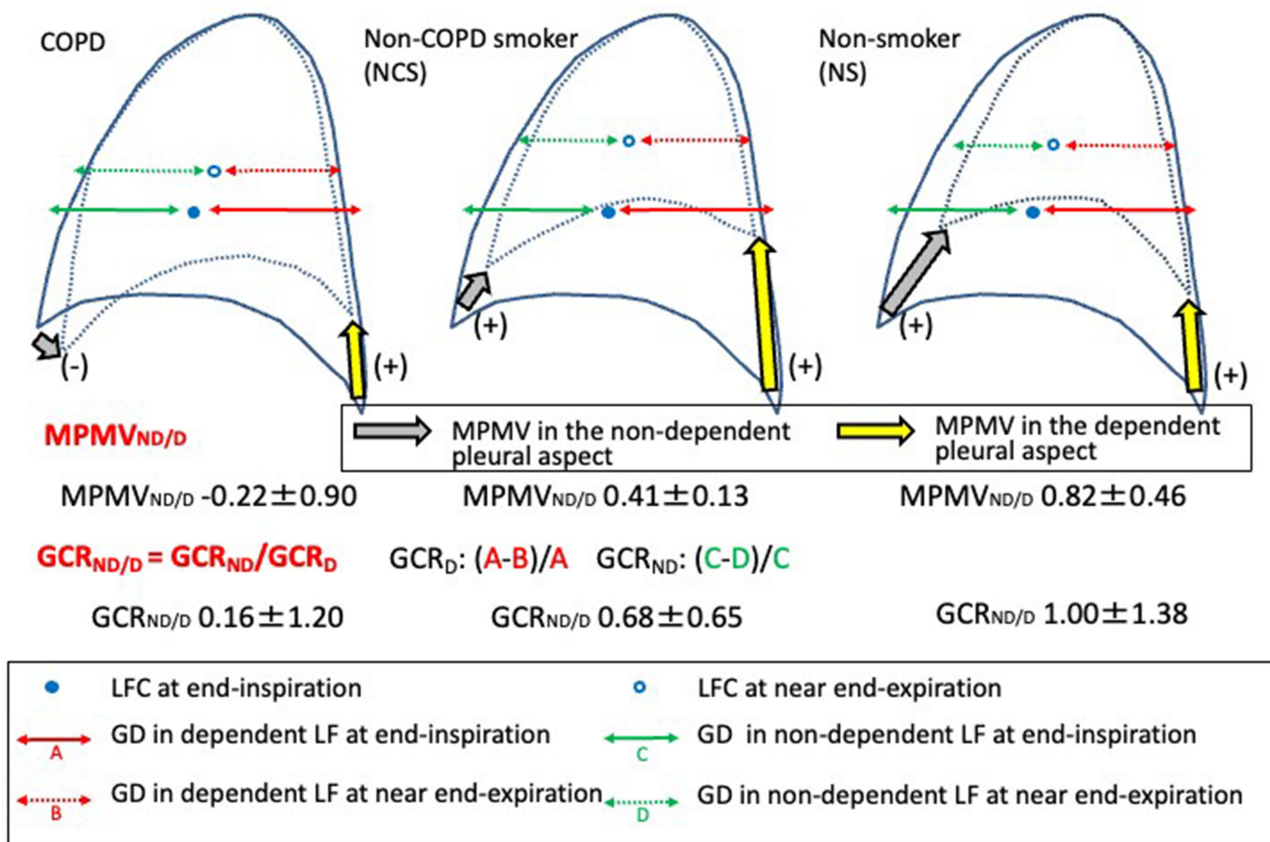


Figure 4 Schematic pleural movements and gravity-oriented parenchymal collapsibility on the median sagittal plane. Schematic overview of differences in pleural movement and gravity-oriented parenchymal collapsibility among the three groups based on our results. MPMV_{ND/D} was smallest in patients with COPD, followed by the non-COPD smoker and non-smoker groups. In addition, values of MPMV_{ND/D} were negative in some patients with COPD. These results indicate that smoking is associated with a relative decrease in the movement of the non-dependent pleural aspect, and air-flow limitation can result in its paradoxical movement. In accordance with this phenomenon, parenchymal collapse during expiration in the gravitational direction for the non-dependent lung field can be impaired in patients with COPD.

Abbreviations: MPMV_{ND/D}, ratio of the non-dependent to dependent pleural aspects in the maximal pleural movement vector; GCR_{ND/D}, ratio of the non-dependent to dependent lung field in the gravity-oriented collapse ratio; LFC, lung field center; GD, gravity-oriented distance.

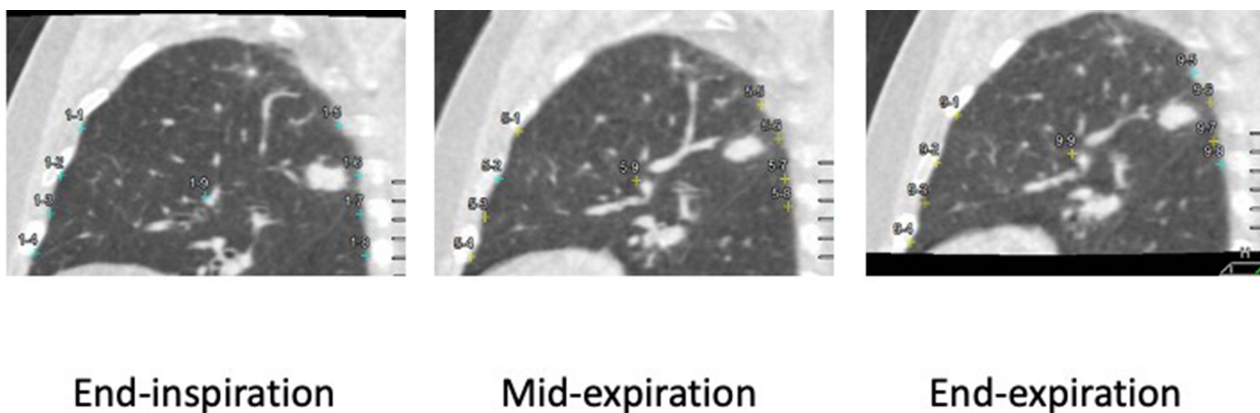


Figure 5 Example images on the median sagittal plane for the left upper lung field for three intermittent time frames in a COPD patient. Median sagittal images for the upper lung field at three intermittent time frames in an 83-year-old male patient with COPD demonstrate smaller movements in the non-dependent pleural aspect compared with the dependent pleural aspect. Moreover, the direction of the movement vector in the non-dependent pleural aspect was caudal. The MPMV_{ND/D} in this case had a negative value of -2.71. Colors of some measurement points on the pleural aspects or the lung field center at end-inspiration changed from blue to yellow at mid-inspiration and end-expiration, which means that these yellow points were located outside the displayed median sagittal plane owing to regional lateral movement.

Abbreviation: MPMV_{ND/D}, ratio of the non-dependent to dependent pleural aspects in the maximal pleural movement vector.

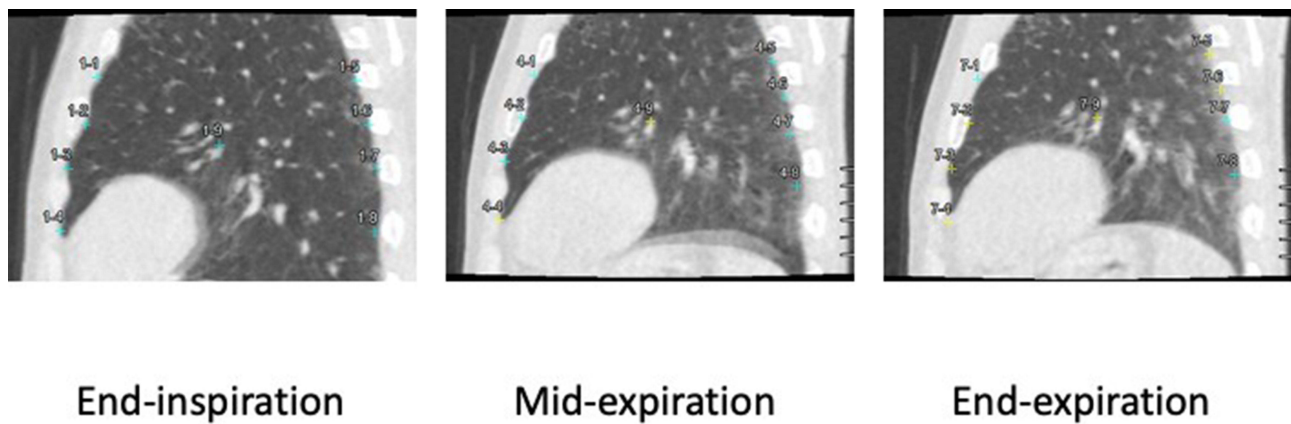


Figure 6 Example images on the median sagittal plane for the left lower lung field for three intermittent time frames in a non-COPD smoker. Median sagittal images for the lower lung field at three intermittent time frames in a 73-year-old male non-COPD smoker demonstrate much smaller movement in the non-dependent pleural aspect compared with the dependent pleural aspect. The $MPMV_{ND/D}$ in this case had a negative value of -0.336 . Colors of some measurement points on the pleural aspect or lung field center at end-inspiration changed from blue to yellow at mid-inspiration and end-expiration, which means that these yellow points were located outside the displayed median sagittal plane owing to regional lateral movement.

Abbreviation: $MPMV_{ND/D}$ ratio of the non-dependent to dependent pleural aspects in the maximal pleural movement vector.

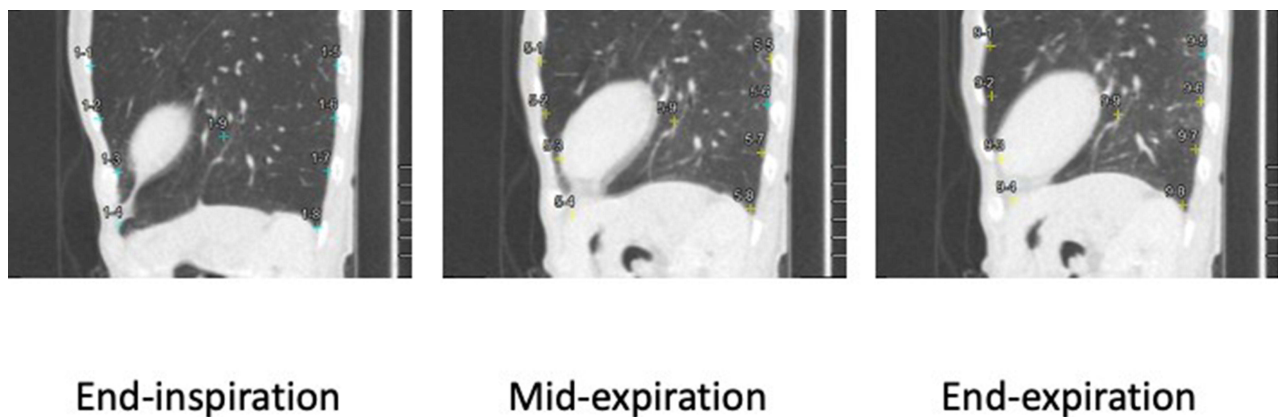


Figure 7 Example images on the median sagittal plane for the left lower lung field for three intermittent time frames in a non-smoker. Median sagittal images for the lower lung field at three intermittent time frames in an 82-year-old female non-smoker demonstrate almost comparable movements in the non-dependent pleural aspect compared with the dependent pleural aspect. The $MPMV_{ND/D}$ in this case had a negative value of -1.24 . Colors of some measurement points on the pleural aspect or lung field center at end-inspiration changed from blue to yellow at mid-inspiration and end-expiration, which means that these yellow points were located outside the displayed median sagittal plane owing to regional lateral movement.

Abbreviation: $MPMV_{ND/D}$ ratio of the non-dependent to dependent pleural aspects in the maximal pleural movement vector.

pulmonary function tests, including the FEV_1/FVC and RV/TLC .^{19,20,26–28} On the other hand, MLD_{CR} tended to correlate with FEV_1/FVC in this study. MLD_{CR} did not show any association with either $FEF_{25–75\%}$ or RV/TLC . Also, neither inspiratory nor expiratory MLD correlated with the respiratory functional indices in this study. These results suggest that MLD_{CR} obtained on 4D-CT does not correspond to total or mid-expiratory airflow, and reflects early expiratory airflow. There are at least two possible causes of this result. First, the inflation level at peak inspiration on 4D-CT may be different from that at deep inspiration in conventional static CT. Second, MLD usually decreases as the ratio of emphysematous changes to total lung fields increases; however, patients with airflow limitation did not necessarily demonstrate apparent emphysematous changes, especially for the airway-dominant subtype. If the number of included cases is large, the proportion of patients with COPD without prominent emphysematous changes tends to be relatively small. In this study, MLD_{CR} also showed a positive correlation with $MPMV_{ND/D}$, which suggested a correlation between the decrease in the maximal rate of lung volume change and reduction in ventral pleural movement; this is a new finding based on data analysis of DVCT.

There are some limitations to this study. First, the total number of enrolled cases was small. Second, we used MLD as an alternative to TLV. DVCT imaging data for the total lung field can theoretically be generated by the feasible combination of data acquired from the upper and lower lung fields separately. Therefore, it will be necessary in the future to examine whether MLD actually correlates with TLV on DVCT in each of the dynamic phases. Third, both $MPMV_{ND/D}$ and $GCR_{ND/D}$ correlated with respiratory functional indices; however, no significant correlation was found between the two measured values. In this study, we used GCR, the distance between LFC and ventral or dorsal pleural aspects, as an index of the gravity-oriented balance in expiratory volume decrease between the dependent and non-dependent lung fields. Although this is a simple index, it is necessary to evaluate whether it is appropriate and whether there may be another, better, quantitative index. We are considering a re-evaluation by measuring regional volume change in lung fields in the future. Fourth, neither MPMV for the ventral aspect nor that for the dorsal aspect was evaluated in this study. Dynamic scanning was performed after the patient's respiratory cycle became constant. Movie images obtained from DVCT demonstrated that inspiratory and expiratory levels during the respiratory cycle varied among patients. Because the absolute value of pleural movement may be strongly affected by individual differences, we adopted $MPMV_{ND/D}$ as an index demonstrating the difference in pleural movement between the ventral and dorsal aspects.

In conclusion, this study demonstrated that $MPMV_{ND/D}$ correlated positively with FEV_1 predicted, FEV_1/FVC , and $FEF_{25-75\%}$, as well as MLD_{CR} , and negatively with the Brinkman index, and $GCR_{ND/D}$ correlated positively with FEV_1 predicted, FEV_1/FVC , and $FEF_{25-75\%}$. These are new findings that need to be recognized when assessing LPA on DVCT.

Acknowledgement

Collaborators Role of the funding Source This study was also arranged as part of the Area-detector Computed Tomography for the Investigation of Thoracic Diseases (ACTIVE) Study, an ongoing multicenter research project in Japan. Each participating institution receives a research grant from Canon Medical Systems. Any other competing interests, such as employment, consultancy, patents, products in development, or marketed products, do not exist regarding this manuscript. The ACTIVE study group The ACTIVE study group currently consists of the following institutions: Osaka Medical College, Takatsuki, Osaka, Japan (Mitsuhiro Koyama, M.D., PhD., Keigo Osuga, M.D., PhD.); Osaka University, Suita, Osaka, Japan (Masahiro Yanagawa, M.D., PhD., Mitsuko Tsubamoto, M.D., PhD., Noriyuki Tomiyama, M.D., PhD.); Fujita Health University, Toyoake, Aichi, Japan (Yoshiharu Ohno, M.D., PhD.); Ohara General Hospital, Fukushima, Fukushima, Japan (Hiroshi Moriya, M.D., PhD.); Tenri Hospital, Tenri, Nara, Japan (Takeshi Kubo M.D., PhD., Satoshi Noma, M.D., PhD.); Yokohama City University, Yokohama, Kanagawa, Japan (Tsuneo Yamashiro M.D.); University of the Ryukyus, Nishihara, Okinawa, Japan (Nanae Tsuchiya, M.D., Akihiro Nishie M.D. PhD.); Kanagawa Respiratory Cardiovascular Center, Yokohama, Kanagawa, Japan (Tae Iwasawa M.D. PhD.); University of Occupational and Environmental Health, Kitakyushu, Fukuoka, Japan (Takatoshi Aoki M.D. PhD.); Urazoe General Hospital, Urazoe, Okinawa, Japan (Sadayuki Murayama M.D. PhD.); Shiga University of Medical Science, Otsu, Shiga, Japan (Ryo Uemura M.D., Yukihiro Nagatani, M.D., Akinaga Sonoda, M.D. PhD., Yoshiyuki Watanabe, M.D., PhD.)

Disclosure

The authors report no conflicts of interest in this work.

References

- Gilmartin JJ, Gibson GJ. Abnormalities of chest wall motion in patients with chronic airflow obstruction. *Thorax*. 1984;39(4):264–271. doi:10.1136/thx.39.4.264
- Iwasawa T, Takahashi H, Ogura T, et al. Influence of the distribution of emphysema on diaphragmatic motion in patients with chronic obstructive pulmonary disease. *Jpn J Radiol*. 2011;29(4):256–264. doi:10.1007/s11604-010-0552-8
- Koyama H, Ohno Y, Fujisawa Y, et al. 3D lung motion assessments on inspiratory/expiratory thin-section CT: capability for pulmonary functional loss of smoking-related COPD in comparison with lung destruction and air trapping. *Eur J Radiol*. 2016;85(2):352–359. doi:10.1016/j.ejrad.2015.11.026
- Farjah F, Wood DE, Mulligan MS, et al. Safety and efficacy of video-assisted versus conventional lung resection for lung cancer. *J Thorac Cardiovasc Surg*. 2009;137(6):1415–1421. doi:10.1016/j.jtcvs.2008.11.035

5. Shimizu H, Endo S, Natsugoe S, et al. Thoracic and cardiovascular surgery in Japan in 2016: annual report by the Japanese association for thoracic surgery. *Gen Thorac Cardiovasc Surg.* 2019;67(4):377–411. doi:10.1007/s11748-019-01068-9
6. Al-Ameri M, Bergman P, Franco-Cereceda A, Sartipy U. Video-assisted thoracoscopic versus open thoracotomy lobectomy: a Swedish nationwide cohort study. *J Thorac Dis.* 2018;10(6):3499–3506. doi:10.21037/jtd.2018.05.177
7. Falcoz PE, Puyraveau M, Thomas PA, et al. Video-assisted thoracoscopic surgery versus open lobectomy for primary non-small-cell lung cancer: a propensity-matched analysis of outcome from the European society of thoracic surgeon database. *Eur J Cardiothorac Surg.* 2016;49(2):602–609. doi:10.1093/ejcts/ezv154
8. Yang CF, Meyerhoff RR, Mayne NR, et al. Long-term survival following open versus thoracoscopic lobectomy after preoperative chemotherapy for non-small cell lung cancer. *Eur J Cardiothorac Surg.* 2016;49(6):1615–1623. doi:10.1093/ejcts/ezv428
9. Byun CS, Lee S, Kim DJ, et al. Analysis of unexpected conversion to thoracotomy during thoracoscopic lobectomy in lung cancer. *Ann Thorac Surg.* 2015;100(3):968–973. doi:10.1016/j.athoracsur.2015.04.032
10. Choong CK, Pasricha SS, Li X, et al. Dynamic four-dimensional computed tomography for preoperative assessment of lung cancer invasion into adjacent structures†. *Eur J Cardiothorac Surg.* 2015;47(2):239–243; 243.
11. Nagatani Y, Takahashi M, Murata K, et al. Lung nodule detection performance in five observers on computed tomography (CT) with adaptive iterative dose reduction using three-dimensional processing (AIDR 3D) in a Japanese multicenter study: comparison between ultra-low-dose CT and low-dose CT by receiver-operating characteristic analysis. *Eur J Radiol.* 2015;84(7):1401–1412. doi:10.1016/j.ejrad.2015.03.012
12. Kim Y, Kim YK, Lee BE, et al. Ultra-low-dose CT of the thorax using iterative reconstruction: evaluation of image quality and radiation dose reduction. *Am J Roentgenol.* 2015;204(6):1197–1202. doi:10.2214/AJR.14.13629
13. Lee SW, Kim Y, Shim SS, et al. Image quality assessment of ultra low-dose chest CT using sinogram-affirmed iterative reconstruction. *Eur Radiol.* 2014;24(4):817–826. doi:10.1007/s00330-013-3090-9
14. Macri F, Greffier J, Pereira F, et al. Value of ultra-low-dose chest CT with iterative reconstruction for selected emergency room patients with acute dyspnea. *Eur J Radiol.* 2016;85(9):1637–1644. doi:10.1016/j.ejrad.2016.06.024
15. Sui X, Meinel FG, Song W, et al. Detection and size measurements of pulmonary nodules in ultra-low-dose CT with iterative reconstruction compared to low dose CT. *Eur J Radiol.* 2016;85(3):564–570. doi:10.1016/j.ejrad.2015.12.013
16. Hashimoto M, Nagatani Y, Oshio Y, et al. Preoperative assessment of pleural adhesion by four-dimensional ultra-low-dose computed tomography (4D-ULDCT) with adaptive iterative dose reduction using three-dimensional processing (AIDR-3D). *Eur J Radiol.* 2018;98:179–186. doi:10.1016/j.ejrad.2017.11.011
17. Nagatani Y, Hashimoto M, Oshio Y, et al. Preoperative assessment of localized pleural adhesion: utility of software-assisted analysis on dynamic-ventilation computed tomography. *Eur J Radiol.* 2020;133:109347. doi:10.1016/j.ejrad.2020.109347
18. Shrimpton PC, Hillier MC, Lewis MA, Dunn M. National survey of doses from CT in the UK: 2003. *Br J Radiol.* 2006;79(948):968–980. doi:10.1259/bjr/93277434
19. Yamashiro T, Matsuoka S, Bartholmai BJ, et al. Collapsibility of lung volume by paired inspiratory and expiratory CT scans: correlations with lung function and mean lung density. *Acad Radiol.* 2010;17(4):489–495. doi:10.1016/j.acra.2009.11.004
20. Xie X, de Jong PA, Oudkerk M, et al. Morphological measurements in computed tomography correlate with airflow obstruction in chronic obstructive pulmonary disease: systematic review and meta-analysis. *Eur Radiol.* 2012;22(10):2085–2093. doi:10.1007/s00330-012-2480-8
21. Mochizuki E, Kawai Y, Morikawa K, et al. Difference in local lung movement during tidal breathing between COPD patients and asthma patients assessed by four-dimensional dynamic-ventilation CT scan. *Int J Chron Obstruct Pulmon Dis.* 2020;15:3013–3023. doi:10.2147/COPD.S273425
22. Yamashiro T, Moriya H, Matsuoka S, et al. Asynchrony in respiratory movements between the pulmonary lobes in patients with COPD: continuous measurement of lung density by 4-dimensional dynamic-ventilation CT. *Int J Chron Obstruct Pulmon Dis.* 2017;12:2101–2109. doi:10.2147/COPD.S140247
23. D'Ascanio M, Viccaro F, Calabrò N, et al. Assessing static lung hyperinflation by whole-body plethysmography, helium dilution, and impulse oscillometry system (IOS) in Patients with COPD. *Int J Chron Obstruct Pulmon Dis.* 2020;15:2583–2589. doi:10.2147/COPD.S264261
24. Pezzuto A, Tralbalza Marinucci B, Ricci A, et al. Predictors of respiratory failure after thoracic surgery: a retrospective cohort study with comparison between lobar and sub-lobar resection. *J Int Med Res.* 2022;50(6):3000605221094531. doi:10.1177/03000605221094531
25. Nagatani Y, Hashimoto M, Nitta N, et al. Continuous quantitative measurement of the main bronchial dimensions and lung density in the lateral position by four-dimensional dynamic-ventilation CT in smokers and COPD patients. *Int J Chron Obstruct Pulmon Dis.* 2018;13:3845–3856. doi:10.2147/COPD.S178836
26. Nagatani Y, Murata K, Takahashi M, et al. A new quantitative index of lobar air trapping in chronic obstructive pulmonary disease (COPD): comparison with conventional methods. *Eur J Radiol.* 2015;84(5):963–974. doi:10.1016/j.ejrad.2014.12.018
27. Akira M, Toyokawa K, Inoue Y, Arai T. Quantitative CT in chronic obstructive pulmonary disease: inspiratory and expiratory assessment. *AJR Am J Roentgenol.* 2009;192(1):267–272. doi:10.2214/AJR.07.3953
28. Lee YK, Oh YM, Lee JH, et al. Quantitative assessment of emphysema, air trapping, and airway thickening on computed tomography. *Lung.* 2008;186(3):157–165. doi:10.1007/s00408-008-9071-0